Multiple Conformations of Physiological Membrane-Bound Cytochrome *c*†

Jorge D. Cortese,* A. Laura Voglino,‡ and Charles R. Hackenbrock

Department of Cell Biology and Anatomy and Laboratories for Cell Biology, The School of Medicine, University of North Carolina, Chapel Hill, North Carolina 27599-7090

Received December 12, 1997; Revised Manuscript Received February 19, 1998

ABSTRACT: One-tenth of cytochrome *c* (cyt *c*) remains bound to the inner mitochondrial membrane (IMM) at physiological ionic strength (*I*; i.e., $I \approx 150$ mM), exhibiting decreased electron transport (ET) activity. We now show that this form of membrane-bound cyt *c* (MB-cyt *c*) can be obtained in vitro and that binding to membranes at low *I* generates an additional conformation with higher ET activity. This low *I* bound form of MB-cyt *c* (MBL-cyt *c*) exhibited intrinsic ET rates similar to those of electrostatically bound cyt *c* (EB-cyt *c*). The ET activity of IMM-bound MB-cyt *c* approached slowly that of MBL-cyt *c* or EB-cyt *c*, suggesting that MB-cyt *c* converts to MBL-cyt *c* while bound to IMM. When maintained at physiological *I*, both forms of MB-cyt *c* were released from the membrane, indicating that they convert to an EB-cyt *c*-like form. This process may be very dynamic in cellular mitochondria, as binding and release for both MB-cyt *c* forms increased considerably with temperature. *I*-Dependent binding of MB-cyt *c* does not require IMM, and it can be reproduced using large or small unilamellar vesicles (SUV). Using SUV−cyt *c* complexes, we characterized the secondary structure of MB-cyt *c* and MBL-cyt *c* by circular dichroism. Conformational analysis revealed that cyt *c* binding as MB-cyt *c* decreases its α-helical content (70−79%) and increases its *β*-sheet up to 135%. The secondary structure of MBL-cyt *c* was similar to that of EB-cyt *c* and soluble cyt *c*, with a modest increase in *β*-sheet. Taken together, our experiments suggest that physiological cyt *c* exists in soluble and membrane-bound conformations with similar ET activity, which may exchange very rapidly, and that soluble hydrophilic proteins can bind transiently to biomembranes.

Cytochrome *c* (cyt *c*),[1] the smallest protein component of the mitochondrial electron transport (ET) carriers, has been considered as a model for electrostatic interactions of peripheral proteins with membranes (*1*−*3*), and it is well established that in the intermembrane space of intact mitochondria (IMS), where the ionic strength (*I*) is similar to that of the cytosol (*4, 5*) and the electrostatic interactions are diminished, cyt *c* diffuses primarily in three dimensions (*6, 7*). However, hydrophobic interactions have been reported to be involved in cyt *c* interactions with membranes (*8, 9*), and a more complex model of cyt *c* binding to membranes is emerging, one where electrostatic and hydrophobic binding forces are implicated. In a previous article (*7*), we reported the existence of a small portion of cyt *c* (MB-cyt *c*) that remains bound to the inner mitochondrial membrane (IMM) under physiological *I* conditions (*4*). MB-cyt *c* has a lower intrinsic ET activity than electrostatically bound cyt *c* (EB-cyt *c*).

In this study, we present evidence that MB-cyt *c* can occur as two distinct conformers with different kinetic properties. Using low (L) *I* for MB-cyt *c* binding to membranes, we were able to initially bind cyt *c* in a stable, high ET activity form (MBL-cyt *c*) that may slowly convert to MB-cyt *c*. We prepared membranes containing predominantly one of these two membrane-associated conformers of cyt *c* and compared their circular dichroism (CD) spectra by performing quantitative analysis of the secondary structure (*10*−*15*). Binding of cyt *c* to membranes has been shown to be very strong and stable, precluding a dynamic exchange with soluble cyt *c* (*16, 17*), but time- and temperature-based release experiments performed by us with both forms of MB-cyt *c* bound to IMM and artificial, liposomal membranes suggest that a very dynamic equilibrium between membrane-bound conformations occurs at physiological *I* and temperature. Our results can be interpreted in a cyclic model, where cyt *c* binds to the IMM surface at physiological *I* in at least two different membrane-bound conformations, which equilibrate with a

† This work was supported by NIH Grant GM-37235 (C.R.H.) and University Research Council Award URC-44758 (J.D.C.).

* To whom correspondence should be addressed: Department of Cell Biology and Anatomy, University of North Carolina at Chapel Hill, 108 Taylor Hall, CB# 7090, Chapel Hill, NC 27599-7090. Telephone: (919) 966−5694. Fax: (919) 966-1856.

‡ Present address: Department of Cell Biology, Duke University, Durham, North Carolina 27710.

[1] Abbreviations: apocyt *c*, apocytochrome *c* (heme-free form of the holoprotein cytochrome *c*); CD, circular dichroism technique; cyt *c*, cytochrome *c*; EB-cyt *c*, electrostatically bound cyt *c*, i.e., cyt *c* that is readily washed from membranes by buffers with high, physiological ionic strength; ET, electron transport; H_{300} medium, 300 mOsm solution composed of 220 mM mannitol, 70 mM sucrose, 2 mM Hepes buffer (pH 7.4), and 0.5 mg/mL BSA.; H*I*B, high ionic strength buffer composed of 50 mM K_2SO_4 containing 2 mM Hepes buffer (pH 7.4); *I*, ionic strength, defined as the ionic concentration $I = (\Sigma c_i z_i^2)/2$, where c_i is the millimolar concentration of the *i*-th ion and z_i is the charge of the *i*-th ion (for salts formed with monovalent ions, e.g., KCl or NaCl, *I* is equivalent to the salt concentration); IMM, inner mitochondrial membranes; IMS, mitochondrial intermembrane space; L*I*B, low *I* buffer, 10 mM NaH_2PO_4, pH 7.4; LUV, large unilamellar vesicles; MB-cyt *c*, membrane-bound cyt *c*, i.e., cyt *c* that is not washed from membranes by buffers with high, physiological ionic strength; MBL-cyt *c*, MB-cyt *c* obtained through binding at low *I*; SUV, small unilamellar vesicles; SVD, singular value deconvolution.

S0006-2960(97)03054-7 CCC: $15.00
Published on Web 04/16/1998

weakly bound EB-cyt *c*-like conformation that is released back into the IMS.

EXPERIMENTAL PROCEDURES

Materials. Antimycin, fatty-acid free bovine serum albumin (BSA), carbonyl cyanide-*m*-chlorophenylhydrazone (CCCP), cholic acid (from ox or sheep bile, sodium salt), horse heart cyt *c* (type VI), rotenone, sodium succinic acid, tetramethyl-*p*-benzoquinone (duroquinone), and *N*,*N*,*N*′,*N*′-tetramethyl-*p*-phenylenediamine (TMPD) were purchased from Sigma Chemical Company (St. Louis, MO). Sephacryl S-200 and Sephadex G-25 were purchased from Pharmacia LKB (Uppsala, Sweden). 3,3′,5,5′-Tetramethylbenzidine (TMBZ) was obtained from Aldrich Chemical Co. (Milwaukee, WI). Asolectin and digitonin were purchased from Calbiochem-Boehringer Corp. (La Jolla, CA).

Preparation of Mitochondrial Membranes. Liver mitochondria were isolated from male Sprague−Dawley rats according to Schnaitman and Greenewalt (*18*) and then resuspended in H_{300} medium. Removal of the outer membrane and purification of the inner membrane/matrix fraction was carried out by controlled digitonin digestion (*19*).

Enrichment of Inner Mitochondrial Membranes (IMM) with Membrane-Bound Cytochrome c (MB-cyt c). We removed electrostatically bound cyt *c* (EB-cyt *c*) from IMM by washing them twice at physiological *I* in 150 mM KCl and 2 mM Hepes (pH 7.4 (*7*)). IMM were resuspended in the KCl-based buffer (10 min at 0 °C) and pelleted (10800*g* for 15 min at 4 °C). We previously demonstrated (*7*) that this protocol washes completely EB-cyt *c* from IMM, giving equivalent results to purification using self-generating Percoll gradients. KCl-washed IMM were incubated at either low *I* (H_{300} medium without BSA) or physiological *I* (150 mM KCl and 2 mM Hepes buffer, pH 7.4), with different bulk concentrations of cyt *c*, and washed several times with physiological *I* medium to remove EB-cyt *c*. When necessary, membranes were incubated in at least a 30-fold dilution of physiological *I* buffer, and aliquots of the suspension were taken at specified times (up to 10 h). Samples from extracted cyt *c* were concentrated, and a lack of proteolysis was verified by specific heme staining of the SDS−PAGE protein band corresponding to cyt *c* (*20*). Multiband patterns typical of proteolyzed cyt *c* were absent (not shown). Samples of MB-cyt *c* were used for quantitative analysis of cyt *c* concentrations by heme spectra (*21*) or to measure specific ET activity by the duroquinol (*22*) or cyt *c* (*23, 24*) oxidase assays previously described (*7*). ET activities were measured polarographically in a Clark oxygen electrode YSI, model 5775, mounted in a Gilson OX-15254 thermostatic chamber (Gilson Medical Electronics, Middleton, WI), as described by Cortese et al. (1995). Electron transport rates are expressed as turnover numbers in units of electrons transferred per second per mole of cytochrome aa_3 (e^-/s/aa_3).

Enrichment of Phospholipid Vesicles with MB-cyt c. Asolectin large unilamellar vesicles (LUV) were prepared by repeated extrusion through polycarbonate membranes (*25*) as described previously (*7*). MB-cyt *c* binding was carried out by exposing the vesicles (15 min at 0 °C) to cyt *c* solutions prepared at either low *I* (H_{300} medium without BSA, pH 7.4) or physiological *I* (150 mM KCl and 2 mM Hepes, pH 7.4), pelleting (105000*g* for 1 h at 4 °C), and resuspending the cyt *c*-containing vesicles twice in 150 mM KCl and 2 mM Hepes (pH 7.4) buffer. Membrane cyt *c* concentration measurements were carried out at specific times (Figure 3), and results are expressed as a protein/lipid molar ratio (micromoles of cyt *c* per mole of phospholipid). Vesicle phospholipid concentrations were estimated as inorganic phosphate (*26*).

MB-cyt *c* binding was also carried out using SUV prepared by ultrasonication according to Cortese et al. (*4*). Repeated membrane binding of cyt *c* at either low or physiological *I* was followed by isolation of MB-cyt *c*-containing SUV by liquid chromatography. SUV containing EB-cyt *c* were prepared by hydrating 0.6 g of asolectin in 3 mL of 10 mM NaH_2PO_4 buffer (pH 7.4; low *I* buffer, or L*I*B) for 2−3 h at 0 °C, followed by 4 cycles of sonication (15 min at 0 °C; *4*). Binding was carried out by adding 1.2 mL of asolectin SUV to 0.8 mL of 10 mM cyt *c* in L*I*B and incubating for 15 min at 0 °C. The sample was then loaded into a Sephacryl S-200 column preequilibrated with L*I*B, and the first peak of EB-cyt *c*-containing vesicles was collected. This fraction was concentrated down to 1 mL in a Centriprep-30 concentrator (Amicon, Inc., Beverly, MA) before use in CD measurements.

To obtain vesicles highly enriched in MB-cyt *c*, asolectin SUV were prepared by hydrating 0.6 g asolectin in 1.5 mL of L*I*B, followed by addition of 1.5 mL of 100 mM K_2SO_4, and 2 mM Hepes buffer (pH 7.4) and sonication as described above. Initial binding was performed by adding 1.2 mL of asolectin SUV to 0.8 mL of 10 mM cyt *c* dissolved in 50 mM K_2SO_4 and 2 mM Hepes buffer (pH 7.4; high *I* buffer, or H*I*B) and incubating for 15 min at 23 °C. Separation of the MB-cyt *c*-containing vesicles was carried out in a Sephacryl S-200 column (H*I*B). After concentration, a new binding step was initiated by addition of 0.8 mL of 10 mM cyt *c* (H*I*B), with subsequent incubation for 15 min at 23 °C, Sephacryl S-200 chromatography (H*I*B) to separate the peak containing MB-cyt *c*, and final concentration. The process was repeated a third time to reach a level of enrichment in MB-cyt *c* appropriate for CD measurements (i.e., approximately 800 μmol of cyt *c* per mole of phospholipid). The MB-cyt *c*-containing vesicles were passed through a fourth column, preequilibrated with L*I*B, to obtain the final preparation destined for CD measurements.

The same protocol was applied to obtain asolectin SUV enriched in MBL-cyt *c*. SUV prepared in L*I*B were exposed to 0.25 mL of 20 mM cyt *c* (L*I*B). A Sephacryl S-200 column (H*I*B) was used to separate EB-cyt *c* from MBL-cyt *c*-containing SUV; the vesicles were diluted 1:4 to decrease bulk *I* and concentrated. These SUV were subjected to two additional consecutive steps of binding of MBL-cyt *c*, liquid chromatography, and concentration. A fourth column run at low *I* (L*I*B) was used to obtain the final preparation of MBL-cyt *c*-containing SUV (L*I*B) used in CD experiments. As with IMM, heme staining was used to verify the absence of cyt *c* proteolysis.

Preparation of Horse Heart Apocytochrome c (apocyt c). We prepared horse heart apocyt *c* from the holoprotein using previously published methods (*27, 28*) adjusted to produce milligrams of the heme-free protein. Ammonium sulfate fractions were kept at −70 °C in small aliquots and thawed and dialyzed against 10 mM NaH_2PO_4 buffer (pH 7.4) containing 0.01% β-mercaptoethanol (4 °C), before use in

CD experiments. This procedure yields 50−60% of the original cyt *c* as apocyt *c*. Complete removal of the heme group in the apoprotein preparation was verified by heme staining (*20*).

CD Measurements. All proteins have similar basic patterns of CD spectra for each type of secondary structure, based in electronic transitions that are rooted in the geometry of the polypeptide skeleton (*29*). Therefore, we cannot analyze cyt *c* when it is bound to a multiprotein system such as the IMM, nor we can separate the contribution of individual membrane-bound forms of MB-cyt *c* as they convert over time. For this reason, CD experiments were carried out with SUV and measurements obtained within 2 h from the time each conformer was bound, conditions under which release of cyt *c* was not detectable (data not shown). Cyt *c* solutions were prepared in a protein concentration range where CD data can be obtained satisfactorily (0.1−0.2 mM). The CD spectra of the soluble protein (holo- and apocyt *c*) and cyt *c*/lipid complexes were recorded at 21 °C using 0.1 mm light path quartz CD cells (Hellma 165-QS; Hellma Cells Inc., Jamaica, NY) in a software-driven Jasco JA-600 spectropolarimeter (Jasco Inc., Easton, MD) while the cuvette chamber was flushed with nitrogen gas. The wavelength range recorded was 182−260 nm, to ensure that we can detect the various β-structures and random coil components of the protein CD spectrum (*13*). We have chosen buffers that give an essentially flat CD spectrum in the experimental wavelength range, using 10 mM NaH_2PO_4 buffer (pH 6.0), L*I*B for low *I* conditions, or the same phosphate buffer with 50 mM K_2SO_4 for physiological *I* (H*I*B).

Appropriate conditions for the collection of CD spectra are known for cyt *c* (*30, 13*). We also followed precautions necessary for obtaining meaningful CD data destined to estimate protein secondary structure down to approximately 184 nm (*12, 13*). For each sample, 16−20 individual spectra were accumulated and averaged to create each spectral data set. Protein concentrations were measured by amino acid analysis (Pico-Tag method (*31*)) using a Waters HPLC instrument. Artifacts arising from light scattering, including absorption flattening (*32*) and differential scattering of incident left and right circularly polarized light (*33*), can affect secondary structure analysis when large particles (i.e., scatterers) such as LUV are present together with the added protein (*34*). We used SUV to diminish those artifacts (*35, 32, 36*). By increasing the protein/lipid ratio through enrichment with MB-cyt *c* as described above, we eliminated these artifacts (cf. spectra of soluble and EB-bound cyt *c* shown in Figure 5). At the low SUV concentrations used in our experiments, their CD spectra were flat in the experimental wavelength range. Protein concentrations for CD spectra obtained from soluble and membrane-bound forms of cyt *c*, and also for apocyt *c*, were calculated as amide bonds. All the spectra were converted to molar ellipticity, or $\Delta\epsilon$ (deg dL mol^{-1} dm^{-1}; ref *12*).

Secondary Structure Analysis. The CD spectra were quantitatively analyzed with two different computer programs that use a database of CD spectra from molecules of known secondary structure (*10, 37, 14, 15*) to deduce the secondary structure of an unknown protein, expressed as the proper fraction of five types of secondary structure: αH, or α-helical; Aβ, or antiparallel β-sheet; Pβ, or parallel β-sheet; Tβ, or β-turns; and OT, or other types of secondary structure, including random coil or aperiodic. The two algorithms were as follows: (a) The variable selection program VARSELE (*10, 11*), which removes a fixed number of protein structures from the reference set and then performs singular value deconvolution (SVD) analysis with each of the possible combinations of the remaining protein structures, until the protein database produces the best fitting of CD parameters. Proteins that make a negative contribution to the goodness of fit are systematically removed until the criteria defined by ref *11* are satisfied. (b) The self-consistency program SELCON (*14, 15*), which also uses the SVD algorithm but adds the unknown protein to the reference set and makes an initial guess of the unknown protein's structure. The extended matrix is then subjected to SVD, and the initial guess is replaced by the solution. The process is repeated until self-consistency is reached. Comparing results from VARSELE and SELCON eliminates any bias introduced by selecting out some of the structures and allows the use of different sets of known proteins. Although we obtained similar results by using VARSELE and SELCON with different protein sets or by using VARSELE with 22- or 30-protein sets, we show here secondary structure values obtained for both programs with the set used by Hennessey and Johnson (*10*).

RESULTS

Electron Transport (ET) Activities of MB-cyt c Forms. The specific ET rate of MB-cyt *c* depended on the ionic strength at which binding to IMM took place. When binding of MB-cyt *c* to IMM was carried out at physiological *I* (*7*), the resulting MB-cyt *c* exhibited about one-third of the activity of cyt *c* electrostatically bound to IMM (EB-cyt *c*; Figure 1A). However, when MB-cyt *c* is bound to IMM at low *I* (MBL-cyt *c*), followed by washes with cyt *c*-free medium at high *I* to remove EB-cyt *c* (see Materials and Methods), it showed specific duroquinol and cyt *c* oxidase activities similar to those of untreated IMM (Figure 1B). Thus, binding of MB-cyt *c* to IMM carried out at low and physiological *I* leads to MB-cyt *c* with different kinetic properties. These kinetically distinguishable forms of MB-cyt *c* are capable of partial interconversion. When IMM enriched in MB-cyt *c* were kept overnight at high *I*, they showed higher specific ET activity, approaching that of untreated IMM (control) kept in low *I* medium to retain all bound cyt *c* molecules (Figure 1C). The duroquinol oxidase activity of control, untreated IMM did not change substantially over the same time period. The same qualitative result is obtained by the cyt *c* oxidase assay (not shown).

Release of MB-cyt c from IMM. Together with the change in specific ET activity shown in Figure 1C, there was also release of the MB-cyt *c* into the high *I* medium. Specific ET activities were measured in the membrane fraction, eliminating contributions from released cyt *c*. We measured MB-cyt *c* contents as a heme *c*/heme *a* ratio, thus correcting for different amounts of protein-containing membrane present in our samples. IMM enriched in MB-cyt *c* or MBL-cyt *c* (Figure 2) were incubated overnight at physiological *I*. There was greater release of MBL-cyt *c* from IMM with respect to MB-cyt *c*. Also, in samples incubated for long periods at high *I*, the dependence of binding on bulk cyt *c* concentration approached that of MB-cyt *c*, becoming proportional to the bulk concentration of cyt *c*. The concen-

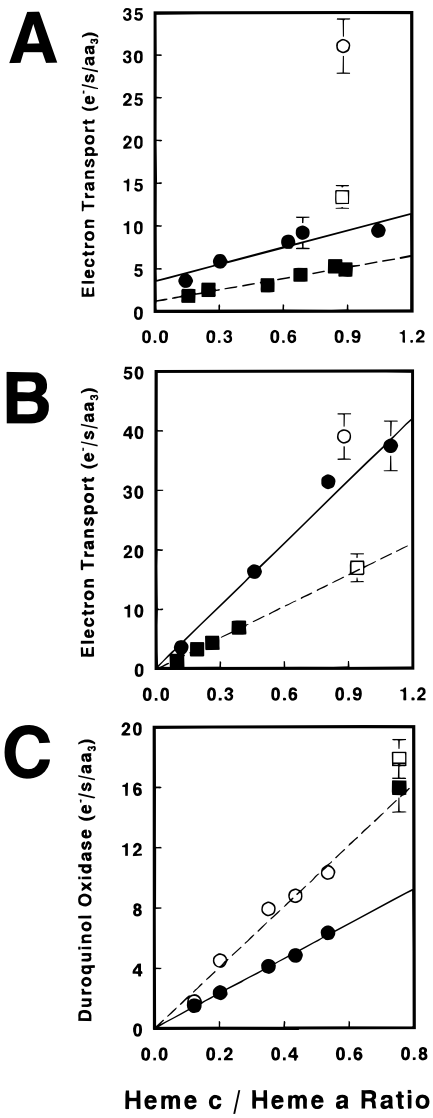

FIGURE 1: Electron transport (ET) activities of MB- and MBL-cyt *c* are shown for duroquinol (■) and cyt *c* oxidase (●). (A) KCl-washed IMM enriched with MB-cyt *c*. ET activities (expressed as mean ± SD) for IMM were 13.4 ± 1.3 $e^-/s/aa_3$ ($n = 5$) for duroquinol oxidase (□) and 31.0 ± 3.2 $e^-/s/aa_3$ ($n = 4$) for cyt *c* oxidase (○). (B) KCl-washed IMM enriched with MBL-cyt *c*. ET activities for IMM were 17.0 ± 2.4 $e^-/s/aa_3$ ($n = 5$) for duroquinol oxidase (□), and 39.0 ± 1.9 $e^-/s/aa_3$ ($n = 4$) for cyt *c* oxidase (○). (C) MB-cyt *c*-enriched membranes were incubated overnight (approximately 15 h) at 21 °C in 145 mM KCl and 2 mM Hepes (pH 7.4). Duroquinol oxidase activity at different heme contents is shown for activities measured in membranes freshly enriched in MB-cyt *c* (●), and after overnight incubation at physiological *I* (15 h; ○). Duroquinol oxidase activities for untreated IMM were, for $t = 0$ h, 15.9 ± 1.6 $e^-/s/aa_3$ ($n = 4$; ■), and for $t = 15$ h, (17.9 ± 1.3) $e^-/s/aa_3$ ($n = 3$; □).

tration dependence of MB-cyt *c* binding did not change substantially with overnight incubation at high *I* (Figure 2). In both cases, an almost linear dependence on the bulk cyt *c* concentration is finally obtained, suggesting that MB-cyt *c* formation is ruled by a single binding probability or partition constant between soluble and membrane-bound states. MBL-cyt *c* was released at a faster rate than that of MB-cyt *c*, suggesting a less stable interaction with the membrane.

Release of MB-cyt c from LUV. MB-cyt *c* can be bound to phospholipid vesicles, also exhibiting *I*-dependent rates

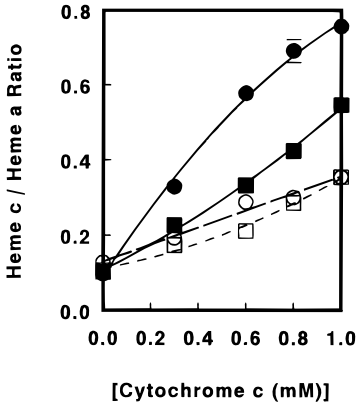

FIGURE 2: Heme *c*/heme *a* ratios were estimated for IMM containing MB-cyt *c* bound at low (●) or physiological *I* (■; $t = 0$ h). Membranes were then incubated overnight ($t = 15$ h) in 150 mM KCl and 2 mM Hepes (pH 7.4), and heme *c*/heme *a* ratios for MBL-cyt *c* (○) and MB-cyt *c* (□) were estimated again after separating soluble cyt *c* by repeated centrifugation in cyt *c*-free medium.

of release. For the same bulk concentration of cyt *c*, binding of MBL-cyt *c* to LUV is greater than that of MB-cyt *c* (Figure 3A). If cyt *c* is bound to asolectin LUV as MB− or MBL-cyt *c* and the MB(L)-cyt *c*-enriched LUV are incubated overnight (approximately 15 h) at physiological *I*, the MBL-cyt *c* contents are reduced by 72% of the initial value, and those of MB-cyt *c*, by 63% (values calculated from the ratio of apparent affinities of the concentration-dependent binding of MB-cyt *c* shown in Figure 3A). Thus, there is a larger fraction of MBL-cyt *c* that can be converted to the weakly bound form of cyt *c* released at physiological *I*. MB-cyt *c* shows a smaller capacity for this conversion. In addition, and as shown for MB-cyt *c* bound to IMM (Figure 2), the release at high *I* of LUV-bound MBL-cyt *c* is faster than that of MB-cyt *c* (Figure 3B). Quantitatively, the exponential release constant of MBL-cyt *c* is 36% greater than that of MB-cyt *c*.

Temperature Dependence of Release Rates. The release rates of MBL- and MB-cyt *c* from membranes increased with temperature (Figure 4). At 4 °C, the MB-cyt *c* content of IMM enriched in MBL- or MB-cyt *c* decreased very slowly over a period of 10 h. Binding of both forms of MB-cyt *c* to LUV is also proportional to the temperature of the initial incubation, as is the amount of MB-cyt *c* remaining on the membranes after prolonged incubation at physiological *I*. The rate of release is also dependent on the ionic strength at which binding is originally carried out (Figure 4), and at physiological *I*, MBL-cyt *c* is released from IMM at a faster rate than MB-cyt *c*. When the exponential decay constants are plotted in a linear representation of absolute temperature (Figure 4, inset), release at 4 °C of MBL-cyt *c* has approximately the same decay constant as that of MB-cyt *c* at 25 °C, and the decay constants of MB- and MBL-cyt *c* only differ by 12% at 25 °C. All samples were compared against a control of IMM washed at physiological *I* from endogenous EB-cyt *c*; its MB-cyt *c* contents did not change over time (not shown). The latter control ensures that the measurement of heme *c* and heme *a* contents on the membranes are not affected during incubation.

Secondary Structures of MB-cyt c Forms. The existence of different membrane-bound conformations of MB-cyt *c* was

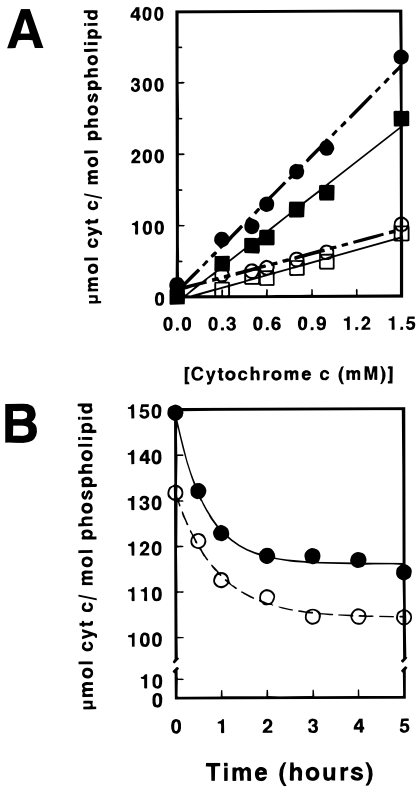

FIGURE 3: (A) Binding of MB- or MBL-cyt *c* to LUV was carried out for various bulk concentrations of cyt *c*. LUV containing various amounts of MB-cyt *c* were incubated overnight (t = 15 h) at physiological I as described in Figure 2. The binding of MB-cyt *c* to vesicles can be represented by a straight line with slope K_{app} (i.e., the apparent affinity of concentration-dependent binding of MB-cyt *c*). For MBL-cyt *c* at t = 0 h (●), K_{app} was 212 mM^{-1} phospholipid (n = 27); at t = 15 h, K_{app} was 57.2 mM^{-1} phospholipid (n = 25) (○). For MB-cyt *c* at t = 0 h (■), K_{app} was 165 mM^{-1} phospholipid (n = 21); at t = 15 h (□), K_{app} 59.7 mM^{-1} phospholipid (n = 21). (B) Time-dependent release from LUV (at 25 °C) for MB-cyt *c* (○) or MBL-cyt *c* (●). Release curves were fitted to the equation cyt *c* (μmol)/phospholipid (mol) molar ratio = $A + B \cdot \exp(-kt\ (h))$; for release of MB-cyt *c*, A = 104, B = 27.5, $k = 1.09 \pm 0.11\ h^{-1}$, and n = 21; and for MBL-cyt *c*, A = 116, B = 33, $k = 1.49 \pm 0.10\ h^{-1}$, and n = 21.

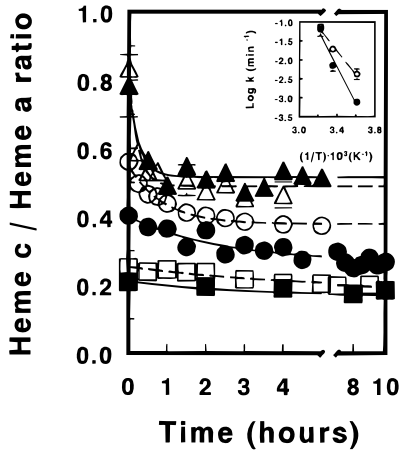

FIGURE 4: IMM containing cyt *c* bound as MBL- or MB-cyt *c* were incubated for variable periods (up to 10 h) in 150 mM KCl and 2 mM Hepes (pH 7.4), and the content of MB-cyt *c* was determined in aliquots that were repeatedly washed in cyt *c*-free medium to remove soluble cyt *c*. Release of MB-cyt *c* from IMM was followed for MBL-cyt *c* (open symbols) or MB-cyt *c* (closed symbols) at 4 (□, ■), 25 (○, ●) and 37 °C (△, ▲). The release was fitted to a single-exponential decay following the equation described in Figure 3. Inset: Arrhenius plot (log k versus reciprocal absolute temperature [1/T]) of the apparent kinetic constants (k) obtained from the release curves for MB-cyt *c* (●) and MBL-cyt *c* (○).

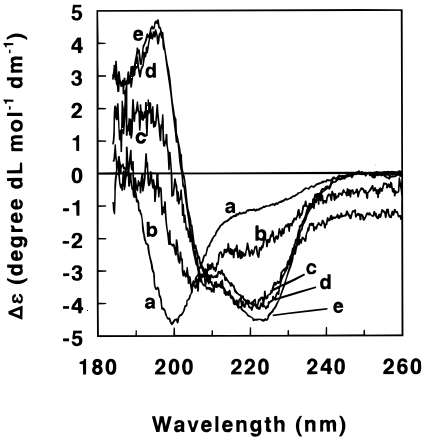

FIGURE 5: Circular dichroism (CD) spectra of (a) apocyt *c*, (b) MB-cyt *c*, (c) MBL-cyt *c*, (d) EB-cyt *c*, and (e) cyt *c* were recorded at 21 °C for the wavelength range 182−260 nm in 10 mM NaH_2PO_4 buffer (pH 7.4) unless otherwise indicated. Data from at least 15 data sets are shown as an average. When CD spectra from samples containing SUV were recorded, i.e., in spectra b, c, and d, a control of the same amount of SUV in buffer was subtracted (using the same number of CD control spectra). Apocyt *c*'s CD spectrum was obtained in 10 mM NaH_2PO_4 buffer (pH 6.0) containing 0.01% β-mercaptoethanol to avoid time-dependent aggregation of the apoprotein.

demonstrated using CD (Figure 5), and by quantitative analysis of the CD spectra (Figure 6). We compared the CD spectra of the heme-free apoprotein (apocyt *c*; Figure 5a) and the soluble, completely folded cyt *c* (Figure 5e) with those of the membrane-bound forms described here. EB-cyt *c* has a very similar CD spectrum to that of soluble cyt *c* (cf. Figure 5, spectra d and e). Also, when the CD spectrum of EB-cyt *c* is normalized as ellipticity (i.e., per mole of average residue), there is no detectable effect of light scattering (coming from absorption flattening or depolarization decreasing the intensity of the CD bands (*38*, *35*)). The CD spectrum of MB-cyt *c* (Figure 5b) shows a decrease in ellipticity values at 222 nm, which is indicative of a loss of α-helical structures (*39*), and overall spectral changes indicative of a increase in β-structures (*29*). An increase in β-structures is also noticeable in the CD spectrum of MBL-cyt *c* (Figure 5c), even though this spectrum is much closer to those of EB-cyt *c* and soluble cyt *c*.

Quantitative analysis of CD spectra of soluble and membrane-bound forms of cyt *c* was carried out by SVD analysis and variable selection (VARSELE; refs *10* and *11*) and by the self-consistent method (SELCON; refs *14* and *15*), revealing the same conformational transition (Figure 6). For purposes of analysis, we included all β-structures into a single column (TOTβ), thus making changes in the extent of α-helical structures and β-structures more apparent. Soluble cyt c and EB-cyt *c* have very similar secondary structures; their values approach those deduced for cyt *c* by X-ray diffraction (38% αH, 0% APβ, 0% Pβ, 17% βT, and 45% OT). The interaction of MB-cyt *c* with the membrane alters substantially its α-helical structures and β-structures. The VARSELE program calculates a 5-fold decrease in αH

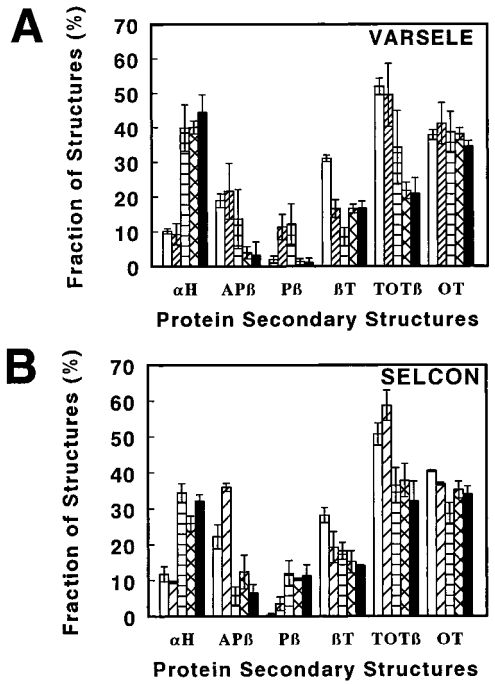

FIGURE 6: CD spectra presented in Figure 5 were quantitatively analyzed using the (A) VARSELE and (B) SELCON algorithms. The analyses give fractional secondary structure contents of the total structure (TOT; theoretically equal to 1.00) for a given level of the root mean square error (rmse) and for 5 types of secondary structure, namely, α-helix, or αH; antiparallel β, or APβ; parallel β, or Pβ; β turns, or βT; and other types, or OT. APβ, Pβ, and βT were pooled as TOTβ. We show results for (i) apocyt *c* (open bar; TOT = 1.01; rmse = 0.10), (ii) MB-cyt *c* (diagonally crossed bar; TOT = 1.00; rmse = 0.27), (iii) MBL-cyt *c* (horizontally crossed bar; TOT = 1.00; rmse = 0.64), (iv) EB-cyt *c* (doubly-crossed bar; TOT = 1.00; rmse = 0.11), and (v) cyt *c* (solid bar; TOT = 1.00; rmse = 0.10).

and a 2.5-fold increase in TOTβ (Figure 6A), and the SELCON program estimates a 3.5-fold decrease in αH and a 2-fold increase in β-structures (Figure 6B). For both programs, αH values are very similar for MBL-cyt *c*, EB-cyt *c*, and soluble cyt *c*. VARSELE (Figure 6A) shows an αH content very similar to that of EB-cyt *c* and soluble cyt *c*. SELCON (Figure 6B) estimates a very small increase of αH (6%) in MBL-cyt *c* with respect to soluble cyt *c*. In the case of β-structures, both programs calculate for MB-cyt *c* a large increase (135% by VARSELE and 82.9% by SELCON). There is some difference in the TOTβ values obtained with both programs for MBL-cyt *c*, but the TOTβ value for MBL-cyt *c* is lower than that for MB-cyt *c*. The OT type of structure (which incorporates aperiodic structures or random coil) is constant throughout all the CD spectra analyzed, including that of apocyt *c*.

The differences between membrane-bound forms of cyt *c* center in variations between α-helical structure and total β-structure (TOTβ). Apocyt *c* and MB-cyt *c* have the highest TOTβ; EB-cyt *c* and soluble cyt *c*, the lowest; and MBL-cyt *c* appears to have an intermediate TOTβ. The α-helical structure shown by MBL-cyt *c* and EB-cyt *c* was similar to that of soluble, compact, and completely folded cyt *c*, but both programs agreed in a small increase in TOTβ for MBL-cyt *c* and EB-cyt *c* with respect to holocyt *c*. Thus, it would appear that formation of MB-cyt *c* involves a disruption of α-helical structure that does not occur during binding of cyt *c* as MBL-cyt *c*, and that the binding of either MB-cyt *c* form causes alterations on the β-structures.

DISCUSSION

Previously, we focused on describing the motional dynamics of cyt *c* in its natural environment, the IMS (*7*). We demonstrated that the IMS has an *I* similar to that of the cytosol (i.e., 100−150 mM; ref *4*), and only a small difference in IMS pH (*5*). Under these conditions, the majority of IMS-cyt *c* diffuses in three dimensions, as evidenced by its motional dynamics studied with resonance energy transfer (*6*). However, our recent study using in vitro membrane binding (*7*) showed that a small fraction of IMS-cyt *c* remains bound to the IMM at physiological *I*. This membrane-bound form of cyt *c* (MB-cyt *c*) exhibits lower intrinsic ET rates. We interpreted this finding as suggesting that cyt *c*, although compactly folded, can partially unfold in contact with membranes. MB-cyt c will then be only a byproduct of the relatively high concentration of soluble IMS-cyt *c*.

We have now studied in greater detail the characteristics of MB-cyt *c*, showing that its binding to membranes is a more dynamic process. The conformation with which cyt *c* binds to membranes and its ability to carry out ET both depend on the ionic strength where binding takes place. Cyt *c* bound as MBL-cyt *c* has ET activity similar to that of electrostatically bound cyt *c* (i.e., EB-cyt *c*), and the molecule possesses a conformation similar to that of native cyt *c*. However, cyt *c* bound at physiological *I* as MB-cyt *c* has a diminished ET capacity. These activities were detected using assays that involve measuring ET via cyt *c* (Complex III → cyt *c* → Complex IV, which constitutes a redox cycle for cyt *c* (*24*)) or *from* cyt *c* (cyt *c* → Complex IV, i.e., measuring ferrocyt *c* oxidation (*23, 24*)), thus comparing cyt *c* activities in both ET protein complexes. From these results and our previous findings (*7*), we concluded that cyt *c* can be bound to IMM in two kinetically distinguishable forms and that membranes enriched in each form can be prepared.

Incubation of MB-cyt *c* at physiological *I* caused changes in ET activity that are consistent with interconversion between MB-cyt *c* (low intrinsic ET rate) and MBL-cyt *c* (high intrinsic ET rate) and also with release of soluble cyt *c* into the bulk medium. This suggests a sequential process whereby MB-cyt *c* converts to a MBL-cyt *c*-like form and, finally, to a EB-cyt *c*-like form that is released from membranes. The same dynamic events can be reconstituted in asolectin LUV, indicating that binding and release of MB-cyt *c* are not dependent on the presence of the ET redox complexes or other IMM proteins. Asolectin phospholipids were used because they represent a membrane interface similar to IMM for cyt *c* (*40, 41*). They also contain less cardiolipin, thus lacking the very high charge density brought about by this phospholipid in artificial membranes frequently used in studies involving cyt *c* (*42, 43*).

In agreement with a sequential (i.e., MB-cyt *c*/MBL-cyt *c*/EB-cyt *c*) conformational transformation of membrane-bound forms of cyt *c* (Figure 7), the release of MBL-cyt *c* from LUV was faster than that of MB-cyt *c*, as was shown for IMM. The rate of release of cyt *c* from IMM increased with temperature, and at 37 °C the process was dominated

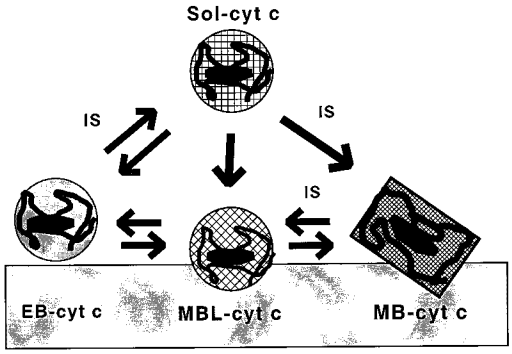

FIGURE 7: A model for the binding and release of cyt *c* from membranes. IS = ionic strength, and Sol-cyt *c* = cyt *c* in solution. MBL-cyt *c*, MB-cyt *c*, and EB-cyt *c* have the meanings used throughout the text. Double arrows indicate processes that can occur in both directions; single arrows, those, such as MB-cyt *c* binding, that we carried out unidirectionally. Some structural deformation of MB-cyt *c* upon membrane binding is also indicated with a different overall shape. The heme group is shown parallel to the plane of the membrane in the forms that are isoactive with soluble cyt *c*, according to most studies of cyt *c* binding to membranes.

by a single kinetic constant (i.e., it became monoexponential). Also, as the temperature approached 37 °C, the differences between the release rates of MB-cyt *c* and MBL-cyt *c* decreased, indicating that both forms can be present in similar amounts at physiological temperature. These results agree with previous binding experiments of liposome-associated and soluble cyt *c* showing that membrane binding is not a rapid equilibrium process (*16*).

CD-based conformational analysis supports the model presented in Figure 7. Different conformations were detected for MB-cyt *c* and MBL-cyt *c*: a more open conformation, with less α-helical structure and more total *β*-sheet for MB-cyt *c*, and an overall conformation for MBL-cyt *c* that is closer to that of EB-cyt *c* and cyt *c*, the latter two being almost identical. The differences in secondary structure of MB-cyt *c* forms may explain their different measured ET activities. Low intrinsic ET rates were detected for MB-cyt *c*, and high ET activity, similar to that of EB-cyt *c*, was detected for MBL-cyt *c*. The model also suggests a transformation that ultimately leads to membrane release of cyt *c*, thus completing a binding cycle in the membrane surface. Our temperature data indicates that the turnover of this cycle could be fast, possibly involving a large fraction of IMS cyt *c* molecules. We conclude from the kinetic and binding data that cyt *c* binds to the membrane at high *I* in a non-native conformation, perhaps by penetrating into a "defect" present in the bilayer surface (*44*), to give a conformation that is not optimal for ET (e.g., because the heme group is not appropriately aligned to carry out ET; (*45, 46*)). MB-cyt *c* can suffer a conformational transition to a nativelike membrane-bound conformation such as MBL-cyt *c*, finally being released from the membrane surface.

Multiple conformations of membrane-bound cyt *c* have been recently suggested by electrochemical and spectroscopic experiments (*17, 47*). These authors support a model where cyt *c* partially or completely penetrates the membrane, leading to redox changes and multiple layers of adsorbed protein. Binding and conformational data presented here reveal a dynamic exchange between membrane-bound conformers of cyt *c*, also supporting the existence of multiple forms of cyt *c*. Our data does not clearly support complete membrane penetration by cyt *c*, which will make the protein capable of crossing a bilayer. Regardless of the specifics of each model, evidence presented here and by Salamon and Tollin (*17, 47*) demonstrates that membrane-bound cyt *c* exists in multiple conformations. This fact may be of importance to understand the process of cyt *c* folding (*48, 2, 49*) and its role in cellular apoptosis (*50, 51*).

There is no simple conformational rule to explain how proteins bind to membrane. For some proteins, α-helices increase (*52, 53, 54*), while for others, *β*-structures are enhanced, upon membrane binding (*55, 56, 57*). The structural transition observed when cyt *c* binds to membranes as MB-cyt *c* shows the loss of α-helices and a significant increment in the *β*-like structures (which appear mainly as AP*β* and P*β* on CD spectra). Penetration to the hydrophobic core requires unfolding into an open structure, explaining the partial loss of α-helical structure. Thus, cyt *c* appears to unfold into a more open structure when bound to membranes, and its transient attachment is then a consequence of the slow reorganization of secondary structures within hydrophobic and packing constraints (*58*). For example, oxidized cyt *c* binds very efficiently to membranes as MB-cyt *c* (*7*), being a more open structure than reduced cyt *c* (*59*).

At high *I*, attenuated electrostatic interactions could lead to tight phospholipid packing (*60*). This would decrease the ability of cyt *c* to penetrate the bilayer, leading to a greater conformational change upon binding as MB-cyt *c*. After partially penetrating a bilayer, MB-cyt *c* will be stabilized by hydrophobic interactions. If the initial interaction with the membrane occurs at low *I*, with a highly charged and less tightly packed surface, MBL-cyt *c* will be formed mainly by deformation of membrane interface, with small changes in protein secondary structure. Accordingly, MBL-cyt *c* is easier to release from the membrane than MB-cyt *c*.

Current debate about cyt *c*'s interactions with membranes centers on the role of membrane-driven unfolding (*61, 43, 49*). The work presented here reveals that intermediate states between the compact, folded and the completely unfolded molecule can exist stably over a period of hours. It shows that even small modifications of secondary structure lead to a long-lived membrane form with intrinsic ET activity similar to that of the native, soluble conformation. Cyt *c* shows considerable conformational flexibility in the presence of membranes, retaining biological activity even when present in conformations that do not closely resemble the native state. Our evidence also points to fast physiological exchange between native, soluble cyt *c* and its membrane-bound analogues, allowing physiological cyt *c* to cycle between a soluble state and others where it behaves as a membrane protein.

Regulation of ET via cyt *c* has been postulated (*62*), as suggested by its binding to GTP (*63*) or ATP (*64*) and to outer membrane channels (*65*). Our work shows that membrane binding of cyt *c* under ionic conditions that are physiological for the IMS renders a complex mixture of membrane-bound forms that differ in intrinsic ET activity. This suggests a putative mechanism for cyt *c*-mediated ET regulation. Accumulation of a MB-cyt *c*-like form of membrane-bound cyt *c* will reduce steady-state ET. Increases in membrane turnover of cyt *c* in a MBL-cyt *c*-like form will affect ET by controlling the extent of three-dimensional diffusion of cyt *c* and by increasing binding to Complexes III and IV. The model of cyt *c* binding to

membranes advanced here and our methodology to prepare and compare the activities of membrane-bound forms of physiological cyt *c* provide a simple framework to test the hypothesis of diffusional regulation of electron transport.

ACKNOWLEDGMENT

The authors thank Dr. Curtiss W. Johnson, Jr. (Oregon State University), for making available to us his structure analysis program VARSELE, and Michael W. Sports for technical assistance with organelle and membrane preparations.

REFERENCES

1. Roder, H., Elöve, G. A., and Englander, S. W. (1988) *Nature 335*, 700−704.
2. Englander, S. W., and Mayne, L. (1992) *Annu. Rev. Biophys. Biomol. Struct. 21*, 243−265.
3. Onuchic, J. N., Beratan, D. N., Winkler, J. R., and Gray, H. B. (1992) *Annu. Rev. Biophys. Biomol. Struct. 21*, 349−377.
4. Cortese, J. D., Voglino, A. L., and Hackenbrock, C. R. (1991) *J. Cell Biol. 113*, 1331−1340.
5. Cortese, J. D., Voglino, A. L., and Hackenbrock, C. R. (1992) *Biochim. Biophys. Acta 1100*, 189−197.
6. Cortese, J. D., and Hackenbrock, C. R. (1993) *Biochim. Biophys. Acta 1142*, 194−202.
7. Cortese, J. D., Voglino, A. L., and Hackenbrock, C. R. (1995) *Biochim. Biophys. Acta 1228*, 216−228.
8. Rietveld, A., Sijens, P., Verkleij, A. J., and de Kruijff, B. (1983) *EMBO J. 2*, 907−913.
9. Szebeni, J., and Tollin, G. (1988) *Biochim. Biophys. Acta 932*, 153−159.
10. Hennessey, J. P., Jr., and Johnson, W. C., Jr. (1981) *Biochemistry 20*, 1085−1094.
11. Manavalan, P., and Johnson, W. C., Jr. (1987) *Anal. Biochem. 167*, 76−85.
12. Johnson, W. C. Jr. (1988) *Annu. Rev. Biophys. Biophys. Chem. 17*, 145−166.
13. Johnson, W. C., Jr. (1990) *Proteins: Struct., Funct., Genet. 7*, 205−214.
14. Sreerama, N., and Woody, R. W. (1993) *Anal. Biochem. 209*, 32−44.
15. Sreerama, N., and Woody, R. W. (1994) *J. Mol. Biol. 242*, 497−507.
16. Rytömaa, M., and Kinnunen, P. K. J. (1995) *J. Biol. Chem. 270*, 3197−3202.
17. Salamon, Z., and Tollin, G. (1996) *Biophys. J. 71*, 848−857.
18. Schnaitman, C., and Greenewalt, J. W. (1968) *J. Cell Biol. 38*, 158−175.
19. Schnaitman, C., Erwin, V. G., and Greenewalt, J. W. (1967) *J. Cell Biol. 32*, 719−735.
20. Goodhew, C. F., Brown, K. R., and Pettigrew, G. W. (1986) *Biochim. Biophys. Acta 852*, 288−294.
21. Williams, J. N., Jr. (1964) *Arch. Biochem. Biophys. 107*, 537−543.
22. Gupte, S. S., and Hackenbrock, C. R. (1988) *J. Biol. Chem. 263*, 5248−5253.
23. Brautigan, D. L., Ferguson-Miller, S., and Margoliash, E. (1978) *Methods Enzymol. 53*, 128−164.
24. Schneider, H., Lemasters, J. J., Höchli, M., and Hackenbrock, C. R. (1980) *J. Biol. Chem. 255*, 3748−3756.
25. MacDonald, R. C., MacDonald, R. I., Menco, B. P. M., and Takeshita, K. (1991) *Biochim. Biophys. Acta 1061*, 297−303.
26. Chen, P. S., Jr., Toribara, T. Y., and Warner, H. (1956) *Anal. Chem. 28*, 1756−1758.
27. Ambler, R. P., and Wynn, M. (1973) *Biochem. J. 131*, 485−489.
28. Hennig, B., and Neupert, W. (1983) *Methods Enzymol. 97*, 261−274.
29. Venyaminov, S. Y., and Yang, J. T. (1996) in *Circular Dichroism and the Conformational Analysis of Biomolecules* (Fasman, G. D., Ed.) pp 69−107, Plenum Press, New York.
30. de Jongh, H. H. J., and de Kruijff, B. (1990) *Biochim. Biophys. Acta 1029*, 105−112.
31. Bennett, H. P., and Solomon, S. (1986) *J. Chromatogr. 359*, 221−230.
32. Glaeser, R. M., and Jap, B. K. (1985) *Biochemistry 24*, 6398−6401.
33. Bustamante, C., Tinoco, I., Jr., and Maestre, M. F. (1983) *Proc. Natl. Acad. Sci. U.S.A. 80*, 3568−3572.
34. Dorman, B. P., Hearst, J. E., and Maestre, M. F. (1973) *Methods Enzymol. 27D*, 767−796.
35. Mao, D., and Wallace, B. A. (1984) *Biochemistry 23*, 2667−2673.
36. Keller, R. C. A., Killian, J. A., and de Kruijff, B. (1992) *Biochemistry 31*, 1672−1677.
37. Toumadje, A., Alcorn, S. W., and Johnson, W. C., Jr. (1992) *Anal. Biochem. 200*, 321−331.
38. Glaser, M., and Singer, S. J. (1971) *Biochemistry 10*, 1780−1787.
39. Chen, Y.-H., and Yang, J. T. (1971) *Biochem. Biophys. Res. Commun. 44*, 1285−1291.
40. Miller, C., and Racker, E. (1976) *J. Membr. Biol. 26*, 319−333.
41. Daum, G. (1985) *Biochim. Biophys. Acta 822*, 1−42.
42. Vincent, J. S., Kon, H., and Levin, I. W. (1987) *Biochemistry 26*, 2312−2314.
43. Spooner, P. J. R., and Watts, A. (1991) *Biochemistry 30*, 3871−3879.
44. Mannella, C. A., Ribeiro, A. J., and Frank, J. (1987) *Biophys. J. 51*, 221−226.
45. Tiede, D. M. (1987) *Biochemistry 26*, 397−410.
46. Pachenche, J. M., Amador, S., Maniara, G., Vanderkooi, J., Dutton, P. L., and Blasie, J. K. (1990) *Biophys. J. 58*, 379−389.
47. Salamon, Z., and Tollin, G. (1997) *J. Bioenerg. Biomembr. 29*, 211−221.
48. Elöve, G. A., Chaffotte, A. F., Roder, H., and Goldberg, M. E. (1992) *Biochemistry 31*, 6876−6883.
49. Pinheiro, T. J. T., Elöve, G. A., Watts, A., and Roder, H. (1997) *Biochemistry 36*, 13122−13132.
50. Adachi, S., Cross, A. R., Babior, B. M., and Gottlieb, R. A. (1997) *J. Biol. Chem. 272*, 21878−21882.
51. Kluck, R. M., Bossy-Wetzel, E., Green, D. R., and Newmeyer, D. D. (1997) *Science 275*, 1132−1136.
52. Cabiaux, V., Brasseur, R., Wattiez, R., Falmagne, P., Ruysschaer, J.-M., and Goormaghtigh, E. (1989) *J. Biol. Chem. 264*, 4928−4938.
53. Holloway, P. W., and Mantsch, H. H. (1989) *Biochemistry 28*, 931−935.
54. Mendz, G. L., Brown, L. R., and Martenson, R. E. (1990) *Biochemistry 29*, 2304−2311.
55. Pezolet, M., Duchesneau, L., Bougis, P., Fauçon, J.-F., and Dufourcq, J. (1982) *Biochim. Biophys. Acta 704*, 515−523.
56. Surewicz, W. K., Moscarello, M. A., and Mantsch, H. H. (1987) *Biochemistry 26*, 3881−3886.
57. Sui, S.-F., Wu, H., Sheng, J., and Guo, Y. (1994) *J. Biochem. (Tokyo) 115*, 1053−1057.
58. Behe, M. J., Lattman, E. E., and Rose, G. D. (1991) *Proc. Natl. Acad. Sci. U.S.A. 88*, 4195−4199.
59. Moser, C. C., and Dutton, P. L. (1988) *Biochemistry 27*, 2450−2461.
60. Romano, R., Dufresne, M., Prost, M.-C., Bali, J.-P., Bayerl, T. M., and Moroder, L. (1993) *Biochim. Biophys. Acta 1145*, 235−242.
61. Spooner, P. J. R., and Watts, A. (1991) *Biochemistry 30*, 3880−3885.
62. Ramasarma, T., Rasheed, B. K. A., Vijaya, S., Puranam, R. S., Shivaswamy, V., Gaikwad, A. S., and Ramakrishna Kurup, C. K. (1992) *Indian J. Biochem. Biophys. 29*, 173−178.
63. Peterson, D. A., and Gerrard, J. M. (1991) *Free Radicals Biol. Med. 11*, 187−190.
64. Wallace, C. J. A. (1993) *FASEB J. 7*, 505−515.
65. Mannella, C. A. (1989) *J. Bioenerg. Biomembr. 21*, 427−437.

BI9730543